

Observations of Self-Focusing Electromagnetic Waves in the Ionosphere

L. M. Duncan^(a)

Department of Space Physics and Astronomy, Rice University, Houston, Texas 77001

and

R. A. Behnke

National Astronomy and Ionospheric Center, Arecibo, Puerto Rico 00612

(Received 5 April 1978)

Self-focusing of high-frequency electromagnetic radiation is observed to produce large-scale plasma striations in the ionosphere. Development of a new observational technique has allowed the first detailed study of the instability scale sizes and associated plasma movement. Experimental results are shown to support the theory of wave self-focusing through differential electron heating.

Natural density fluctuations cause small variations in the index of refraction of a plasma, resulting in a slight focusing and defocusing of an electromagnetic wave as it propagates through the medium. The electric field intensity increases as the incident wave refracts into regions of comparatively underdense plasma. Ohmic heating¹ and the electric-field ponderomotive force² then drive plasma from these focused regions, amplifying the initial perturbation. This self-focusing instability continues until hydrodynamic equilibrium is reached, creating field-aligned striations within the plasma.

The study of self-focusing waves in plasmas is motivated by its relevance to ionospheric modification research,³ laser fusion-plasma heating,⁴ and microwave-ionosphere interactions associated with solar-power satellite systems.⁵ Development of a new diagnostic technique in conjunction with a recent ionospheric modification experiment has resulted in the first detailed observations of individual self-focused striations, as well as striation maps of the entire wave-plasma interaction region. Measured striation scale sizes are in good agreement with the predictions of thermal self-focusing theory. Additional plasma effects can also be identified.

Intense, high-frequency (hf) electromagnetic radiation incident on an overdense ionospheric plasma is known to excite parametric instabilities, enhancing electron plasma oscillations observable by incoherent backscatter radar.⁶ These instabilities continue to be the subject of intense experimental study. Of importance here is the fact that above instability threshold the strength of the enhanced plasma waves directly depends on the local power of the pump electric field. In addition, because of exact frequency and wave-number matching conditions for both the parametric wave-plasma interaction and the radar in-

coherent backscatter process, these enhanced waves are detected at only one altitude. As a result, systematic scanning of the narrow radar beam across the interaction region of the enhanced plasma waves yields a two-dimensional cross-section characteristic of the local electric field intensity. These maps of electric field strength clearly show self-focusing striations and large-scale structuring of the illuminated plasma. Because the direction and rate of the radar scan are experimentally controlled, the cross-sectional dimensions of the individual striations are easily measured. Alternatively, if the radar is fixed, the irregularities follow a slow natural ($\vec{E} \times \vec{B}$) drift through the beam, allowing a detailed study of the small-scale structure within individual striations. Once the irregularity size is determined, striation velocities can be calculated from these drift measurements. The ex-

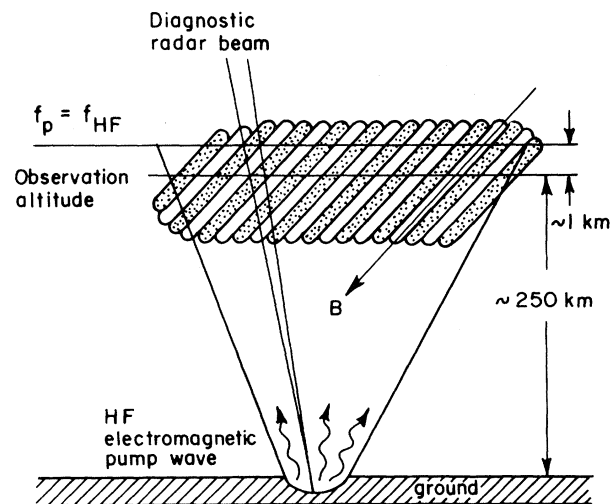


FIG. 1. The experimental configuration for incoherent backscatter radar mapping of plasma striations, attributed to self-focusing of electromagnetic waves in the ionosphere.

perimental configuration is shown in Fig. 1.

The data presented here were obtained during an ionospheric modification experiment conducted from 2 June to 17 June 1977 at the Arecibo Observatory (NAIC). The incoherent backscatter radar operates at 430 MHz with a $\frac{1}{6}^\circ$ beamwidth, corresponding to approximately 730 m at a typical interaction height of 250 km. The hf-wave beamwidth is a function of the operating frequency, ranging from 7.2° at 7.8 MHz to 10.9° at 5.185 MHz, or beam diameters of 31.5 and 47.5 km, respectively, at 250-km altitude. The hf radiation is transmitted continuously with ordinary polarization and is fixed at vertical incidence, while the 430-MHz radar is pulsed and can be swept in zenith angle at a maximum rate of $1.87^\circ/\text{min}$, or 136 m/sec at 250 km. The en-

hanced plasma-wave intensities are measured over a 20-kHz bandwidth offset from 430 MHz by the hf pump frequency. A 500- μsec radar pulse is used with a pulse repetition period of 8500 μsec , as determined by the 6% transmitter duty cycle. The data rate is not continuous; data are accumulated in arrays of 1024 pulses, after which there appears a data gap of approximately 0.4 sec in which the array is displayed in real time and recorded on magnetic tape.

Results of the two basic observational strategies are shown in Fig. 2. The data in Fig. 2(a) represent the natural drift of striations through the fixed radar beam. This drift gives rise to a slow regular modulation of the measured plasma line intensities, with typical periods of 60 to 90 sec. Similar fluctuations have been noted previ-

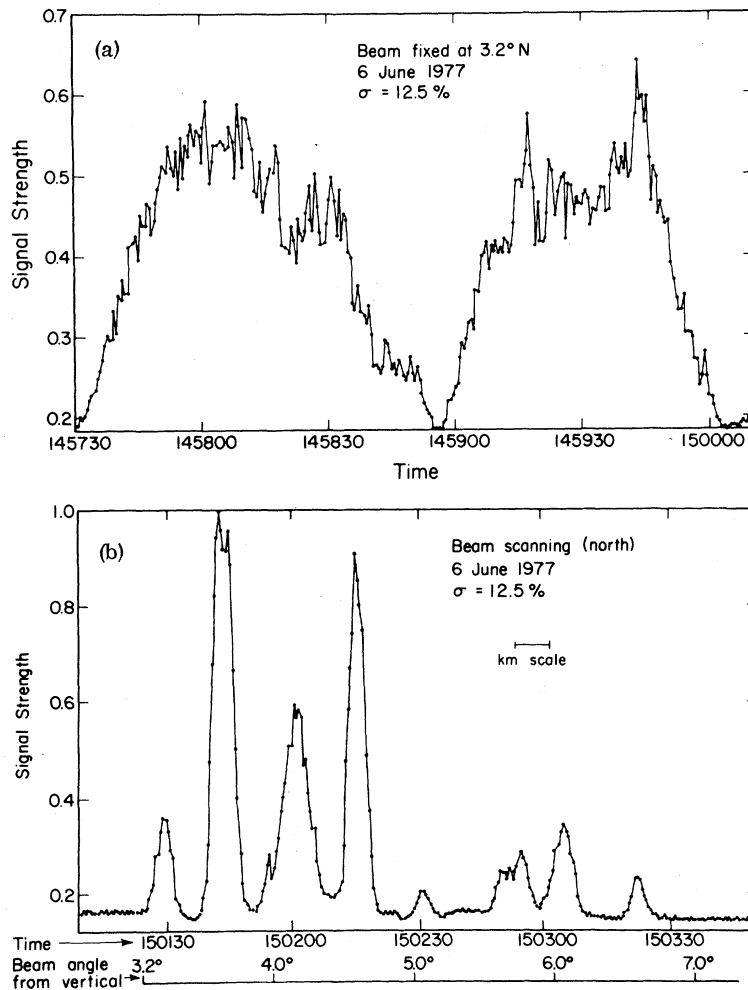


FIG. 2. (a) Signal modulation induced by the natural drift of striations through the fixed radar beam. The units of signal strength are normalized consistent with (b). (b) A series of striations as observed from rapid scanning of the radar beam across the interaction region immediately after the drift measurements shown in (a). The striations can be measured from the sweep time of the radar beam, in terms of the angle from vertical incidence of the beam, or as kilometers at the altitude of excitation.

ously without interpretation.⁷ The second data set Fig. 2(b), was taken immediately following the above drift measurements and shows a series of distinct striations observed by rapidly sweeping the radar beam north across the interaction region. Typical striation dimensions deduced from observations over many such scans are 1.2 km in the north-south plane and 1.0 km in the east-west plane. Striation velocities are on the order of 25 m/sec, with components of 20 m/sec to the east, and smaller than 15 m/sec in the north-south direction. North-south velocity measurements are complicated by the strong spatial dependence of the striation width in the magnetic meridian plane.

A useful observing procedure is to scan the radar through a set of striations, quickly reverse the beam direction, and sweep back through the same striations. This yields a simultaneous determination of striation size and velocity in the scan direction. An example of data taken using this technique is shown in Fig. 3. The striation widths and relative spacings are significantly affected by scanning with or against the component of the striations' drift motion. The data shown here clearly suggest a dominant drift movement to the east. The striation dimensions then can be calculated including a correction for velocity-induced measurement errors as well as allowing for the radar beamwidth. The lower limit for striation sizes thus measured is approximately 500 m.

The experimental observations are best explained by thermal self-focusing theory.¹ Self-focusing driven by the ponderomotive force has

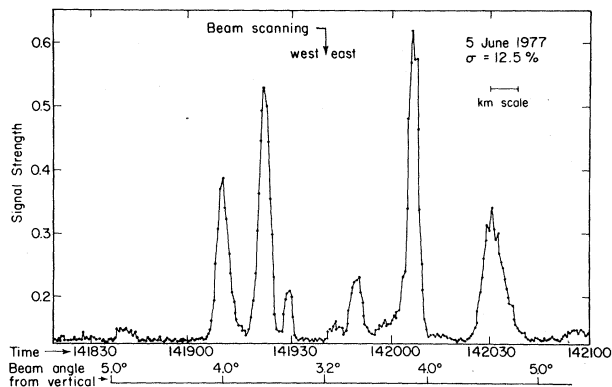


FIG. 3. A westward scan of a compact striation set, reversal of sweep direction at 141940, and an eastward scan back through the same striations. To facilitate comparisons the units of signal strength once again have been normalized to Fig. 2(b).

been shown to occur at higher power fluxes than thermal self-focusing.⁸ For the conditions appropriate to an overdense ionospheric modification experiment, the thermal-instability threshold field is given by¹

$$\epsilon_0^2 c / 8\pi = 2c T_e \kappa (k \sin \theta)^2 / \nu_e k_0 L,$$

where ϵ_0 is the electric field amplitude of the incident wave, T_e is the electron temperature ($^{\circ}\text{K}$), κ is the thermal conductivity, k is the wave vector perpendicular to the propagation direction, θ is the angle between the wave propagation direction and the magnetic field, ν_e is the electron collision frequency, $k_0 = 2\pi f/c$, where f is the incident wave frequency, and L is the plasma scale height. In terms of experimental parameters the threshold power flux can be expressed as

$$P_{\text{thres}} (\text{W}/\text{m}^2) \approx (1.9 \times 10^{12}) T_e^{-5} \sin^2 \theta / L f_{\text{hf}}^3 \lambda^2,$$

where f_{hf} is the incident pump-wave frequency and λ is the excited striation width. For typical experimental conditions at an altitude of 250 km, $T_e = 1200^{\circ}\text{K}$, $L = 100$ km, $f_{\text{hf}} = 8$ MHz, and $\theta = 40^{\circ}$ (vertical incidence at Arecibo), then

$$P_{\text{thres}} (\text{W}/\text{m}^2) \approx 38\lambda^{-2}.$$

The hf power flux at 250 km can be estimated at $30 \mu\text{W}/\text{m}^2$, yielding a striation width of $\lambda = 1.1$ km. This agrees well with the experimentally measured values. However, the self-focusing theory predicts that striations with widths 1.1 km and greater should develop. Apparently the saturation state of the self-focusing instability preferentially selects for growth the smallest λ compatible with a given P_{thres} . In the east-west plane the striation widths are predicted to be approximately 500 m,⁹ again in relative agreement with the observations.

A more detailed comparison of experimental and theoretical striation dimensions is given in Fig. 4. The pump power density is taken to be a Gaussian distribution across the hf beam, causing the theoretically predicted striation width to increase with angle from vertical incidence. Additionally, in the magnetic meridian (north-south) plane, the angle between the hf-wave vector and the magnetic field also is a function of beam angle from vertical incidence. These effects are combined to produce the theoretical curves shown in Fig. 4, which again approximate the experimental data very well.

An unusual feature of the experimental observations is the tendency of the striations to appear

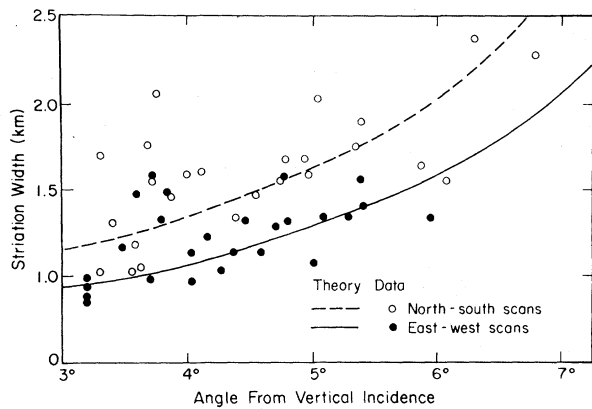


FIG. 4. Variation of plasma striation width as a function of beam angle from vertical incidence: experimental results and thermal self-focusing theoretical predictions.

in sets of 2 to 4, e.g., Figs. 2(b) and 3. No explanation is offered for this large-scale envelope structuring of the interaction region. Density perturbations $\Delta\eta_e$ due to the field self-focusing are estimated at about 5% of the natural background density η_e . This implies that the plasma density profile within a striation is shifted upwards by

$$\Delta x \approx \Delta\eta_e L / \eta_e \approx 5 \text{ km} \quad (3)$$

with respect to the natural density profile. This result then offers a simple explanation for the similar height difference recently observed between natural photoelectron-enhanced plasma waves and the parametrically enhanced waves,¹⁰ which are shown here to be produced in a striated plasma.

The results presented here provide an important experimental verification of thermal self-focusing theory over the range of parameters applicable to ionospheric modification experiments. The confirmation of predicted scaling laws supports extrapolations of self-focusing theory to laser fusion research and studies of solar-power-satellite microwave-beam/ionosphere interactions.¹ In addition, the detection and observation

of induced plasma striations in the ionosphere has led to a much improved understanding of the overall ionospheric modification experiment, yielding insights into the sources of other observed phenomena which were previously unexplained.

The ionospheric heating experiments described in this paper were performed with the scientific collaboration of W. E. Gordon from Rice University and F. W. Perkins from Princeton University. We thank the team of heating coexperimenters and the Arecibo Observatory staff for their cooperation and assistance. The Arecibo Observatory is operated by Cornell University under contract to the National Science Foundation. This work was partially supported by the Atmospheric Research Section, National Science Foundation, under the National Science Foundation Grant No. ATM76-15550.

^(a)Current address: Los Alamos Scientific Laboratory, Los Alamos, N. M. 87545.

¹F. W. Perkins and E. J. Valeo, *Phys. Rev. Lett.* **32**, 1234 (1974); B. S. Abramovich, *Izv. Vyssh. Uchebn. Zaved., Radio Fiz.* **19**, (1976) [*Radiophys. Quant. Elect.* **19**, 231 (1977)].

²A. G. Litvak, *Zh. Eksp. Teor. Fiz.* **57**, 629 (1968) [*Sov. Phys. JETP* **30**, 344 (1970)].

³T. M. Georges, *J. Geophys. Res.* **75**, 6436 (1970); G. D. Thome and F. W. Perkins, *Phys. Rev. Lett.* **32**, 1238 (1974).

⁴K. A. Brueckner, *IEEE Trans. Plasma Sci.* **1**, 13 (1973); J. Nuckolls, J. Emmett, and L. Wood, *Phys. Today* **26**, No. 8, 46 (1973); L. C. Johnson and T. K. Chu, *Phys. Rev. Lett.* **32**, 517 (1974).

⁵W. C. Brown, *IEEE Spectrum* **10**, 38 (1973).

⁶H. C. Carlson, W. E. Gordon, and R. L. Showen, *J. Geophys. Res.* **77**, 1242 (1972); A. Y. Wong and R. J. Taylor, *Phys. Rev. Lett.* **27**, 644 (1971).

⁷I. J. Kantor, *J. Geophys. Res.* **79**, 199 (1974).

⁸F. W. Perkins, *Bull. Am. Phys. Soc.* **18**, 1335 (1973).

⁹B. L. Cragin and J. A. Fejer, *Radio Sci.* **9**, 1071, (1974); R. L. Berger, M. V. Goldman, and D. F. DuBois, *Phys. Fluids* **18**, 207 (1975); B. L. Cragin, J. A. Fejer and E. Leer, *Radio Sci.* **12**, 273 (1977).

¹⁰D. B. Muldrew and R. L. Showen, *J. Geophys. Res.* **82**, 4793 (1977).